END
DATE
FILMED
8 85
DTIC

RFD-4164-AN

②

IMPERIAL COLLEGE OF SCIENCE AND TECHNOLOGY

DEPARTMENT OF MECHANICAL ENGINEERING

FLUIDS SECTION    LONDON SW7 2BX

THE FLOW OF DILUTE SUSPENSIONS OF PARTICLES AROUND AXISYMMETRIC BAFFLES

by

J.M. Nouri, J.H. Whitelaw and M. Yianneskis

DTIC
S ELECTE D
JUL 2 9 1985

June 1984

FS/84/18

85   7  16  025

## 1. INTRODUCTION

This report presents an experimental investigation of the mean flow and turbulence characteristics of the two-phase (liquid-solid) flow around axisymmetric baffles. Flows of particle suspensions attract considerable interest because of the diversity of engineering applications in which they are encountered; the confined flow around a baffle is one such example and provides the opportunity of investigating the particle behaviour in the recirculation zone behind the baffle as well as in the jet flow downstream of the recirculation.

Information on two-phase flow around baffles is scarce, but the properties of suspensions of solids in fluids have been examined for a variety of configurations and some of the studies relevant to the present work are summarised in Table 1.

The presence of solid particles may alter the properties of the bulk flow and significantly affect the properties of the carrier phase. An increase in the volume fraction of solids is expected to cause an increase in pressure drop and friction factor, although the suspension may become non-Newtonian for high particle concentrations and result in reduced pressure loss as compared to single-phase flow (Soo, 1967). Interaction between particles varies with concentration and values of 2% volume fraction (Steinour, 1944) or even as low as 0.5% (Kaye and Boardman, 1962) have been suggested as limits above which particle interactions cannot be ignored. Kaye and Boardman point to the existence of different regimes of particle settling for different solids concentrations and in particular to the formation of clusters with increased terminal velocities in dilute suspensions.

Soo et al (1964) observed that the mean velocity profile of the continuous phase is unaltered by the presence of solid particles of 20-150um diameter in air for mass loadings of up to 8.0, while Cox and Mason

TABLE 1 - Previous experimental investigations of the velocity characteristics of two-phase flows

$\bar{v}_{f,1}$, $\tilde{v}_{f,1}$: mean and r.m.s. velocity of fluid in single-phase flow    $d_p$: particle (or droplet) diameter

$\bar{v}_{f,2}$, $\tilde{v}_{f,2}$: mean and r.m.s. velocity of fluid in two-phase flow

$\bar{v}_p$, $\tilde{v}_p$: mean and r.m.s. velocity of the dispersed phase in two-phase flow

| Authors; Year | Flow Configuration | Particle Size(s) | Particle Concentration by Volume | Mass Loading | Main Findings |
|---|---|---|---|---|---|
| Hetsroni and Sokolov; 1971 | Horizontal air-liquid droplet axisymmetric turbulent jet | 13μm mean droplet diameter | $(2.16-7.97) \times 10^{-6}$ | - | 2-phase mean and r.m.s. velocities found to be about 10% and 20-40% respectively less than single-phase ones; suppression of turbulence found to be proportional to concentration |
| Einav and Lee; 1973 | Liquid-solid boundary layer flow in a channel | 30,50 and 100μm | 0.4 and $6 \times 10^{-2}$ | - | Migration of particles away from the wall was observed in the boundary layer |
| Birchenough and Mason; 1976 | Upward gas-solid flow in a vertical pipe of 50mm diameter | 5-45μm | - | 0-2.0 | $\bar{v}_p$ increased as mass loading was increased; $\bar{v}_p$ profiles were flatter and about 10% smaller in magnitude than $\bar{v}_{f,1}$; $\tilde{v}_p$ varied significantly with mass loading |
| Zisselmar and Molerus; 1978 | Liquid-solid flow in a horizontal pipe of 50mm diameter | 53μm | $0-5.6 \times 10^{-2}$ | | Turbulence was suppressed in the presence of particles by 12-40% for concentrations of 1.7-5.6% correspondingly |
| Levy and Lockwood; 1981 | Downward flowing unconfined gas-solid jet of 15mm exit diameter | 215,400, 540,725 and 1060μm | - | 1.14-3.5 | Spread of jet affected by particle size and concentration; $\bar{v}_p$ profiles flatter than $\bar{v}_f$ ones; $\tilde{v}_{f,2}>\tilde{v}_{f,1}$ for 1060μm particles, $\tilde{v}_{f,2}<\tilde{v}_{f,2}$ for 215μm particles and $\tilde{v}_{f,2}\approx\tilde{v}_{f,1}$ for all other sizes; $\tilde{v}_f>\tilde{v}_p$ |
| Lee and Durst; 1982 | Upward gas-solid flow in a vertical pipe of 20.9mm diameter | 100, 200, 400 and 800μm | $0-1.21 \times 10^{-3}$ | - | $\bar{v}_p$ profile became flatter as $d_p$ increased; particle-free region near wall observed for the 400 and the 800 μm particles; $\tilde{v}_{f,2}<\tilde{v}_{f,1}$ for $d_p<400$μm and $\tilde{v}_{f,2}\approx 2.0$ $\tilde{v}_{f,1}$ for 800μm ones |
| Modarress et al; 1982 | Downward gas-solid flow in a confined jet of 20mm exit diameter | 50 and 200μm | $0-3 \times 10^{-4}$ | 0.64 | $\bar{v}_p$, $\tilde{v}_{f,2}>\tilde{v}_{f,1}$ and $\tilde{v}_{f,2}<\tilde{v}_{f,1}$ for 200μm particles; $\tilde{v}_{f,1}$ profiles were flatter than $\bar{v}_{f,2}$ ones |
| Tridimas et al; 1982 | Upward gas-solid flow in vertical pipes of 22,25.8 and 31.4mm diameters | 40 - 1000μm | - | - | $\bar{v}_p$, $\tilde{v}_{f,2}<\tilde{v}_{f,1}$ for most particle sizes; $\tilde{v}_p>\tilde{v}_{f,1}$ but $\tilde{v}_{f,2}<\tilde{v}_{f,1}$ for all particle sizes |
| Tsuji and Morikawa; 1982 | Gas-solid flow in a horizontal pipe of 30.5mm | 200 and 3400μm | $0-4 \times 10^{-3}$ | 0-6.0 | 200μm particles suppressed turbulence but 3400μm ones augmented it; $\bar{v}_p$, $\tilde{v}_{f,2}$ profiles more uniform than $\bar{v}_{f,1}$ ones |
| Wells and Stock; 1983 | Gas-solid flow behind a grid in a channel | 5 and 57μm | - | - | 5μm particles did not affect the flow but $\bar{v}_p\approx 0.6\bar{v}_{f,1}$ in the case of the 57μm particles |
| Tsuji et al; 1984 | Upward gas-solid flow in a vertical pipe of 30.5 | 200 - 3500μm | - | 0-5.0 | $\tilde{v}_{f,2}$ profiles were flatter than $\bar{v}_{f,1}$ ones and $\bar{v}_p$ profiles flatter than $\tilde{v}_{f,2}$ ones; for $d_p=200$μm, $\bar{v}_p>\tilde{v}_{f,2}$ near the wall; $\tilde{v}_{f,2}>\tilde{v}_{f,1}$ for $d_p>500$μm, and $\tilde{v}_{f,2}<\tilde{v}_{f,1}$ for $d_p=200$μm |

(1975) reported identical fluid and particle velocities for neutrally buoyant solids in low to moderate concentrations. Einav and Lee (1973) reported small differences in the liquid phase velocity profile in laminar flow with increasing concentration of up to 6% by volume and also found that the relative velocity between the two phases decreased as the particle concentration increased. Particle size was not found to have any significant effect on the mean flow, but both the size and the concentration of solids is reported to influence the turbulence structure (Soo, 1967). Einav and Lee point also to the importance of the near-wall region and the existence of particle-free areas in its vicinity. Tsuji and Morikawa (1982) found that in dilute air-solid pipe flow 0.2mm diameter particles flattened the velocity profile and suppressed turbulence, while 3mm diameter particles increased turbulence significantly.

As shown in Table 1, most studies are restricted to air flows with very low concentrations of solids, which is primarily a result of the experimental difficulties arising at higher particle densities (laser anemometer beam blockage, probe blockage or damage, etc.). The complexity of the flow processes and the presence of the solid particles constitute significant difficulties for the calculation and measurement of liquid-solid flows. The majority of relevant experimental work has been carried out in gas-solid flows and in flows with concentrations below 1%; data for situations with high content of solids are limited to pressure drop characteristics mainly (see e.g. Abbott, 1955). Various theoretical treatments have been proposed for the flow of suspensions and a review of them is given by Lee and Durst (1982). Grossman (1981) has formulated equations for neutrally buoyant solid sphere suspensions of moderate concentrations, characterising the flow by a macroscopic coefficient of viscosity. Choi and Chung (1983) calculated dilute gas two-phase flow in a pipe by considering the solid phase to behave as a secondary fluid mixed with the primary fluid. Owen (1969) estimated that the rate of turbulent

energy dissipation in a fluid containing small particles is greater by $(1\pm\rho_p/\rho_f)$ and the turbulence intensity is smaller by $(1+\rho_p/\rho_f)^{-1/2}$ than in a particle free fluid, where $\rho_p$ is the mass of particles per unit volume.

The presence of the suspended solids suggests that the application of non-obtrusive optical techniques is necessary for the measurement of the velocity characteristics. Laser-Doppler anemometry has been employed successfully for the measurement of two-phase flows, but the blocking of the beams and of the scattered light by the solid particles has limited its application to dilute flows. In addition, the need to distinguish between signals from the two phases necessitates the use of expensive electronic processing equipment. Various methods have been suggested for phase discrimination, and are based mainly on the electronic filtering and differentiation of the a.c. and d.c. components of the Doppler signal (see e.g. Einav and Lee, and Tsuji and Morikawa).

In the present work an optical technique is employed to distinguish the solid-phase velocities, which are compared to the liquid-phase velocities in the absence of particles. In order to maintain axial symmetry and avoid concentration gradients in the flow, acrylic plastic particles of 270$\mu$m mean diameter that were neutrally buoyant were chosen. The velocities of the particles in the flows behind a conical baffle of 25% pipe area blockage and a disc-shaped baffle of 50% pipe area blockage were measured for a solids concentration of 0.375% by volume and the effect of increasing concentration up to 1.5% was examined.

The flow configurations and the experimental apparatus are described in the following sub-section. The laser-Doppler anemometer and the measurement technique are described and an assessment of the measurement precision is given in sub-section 2.2. The mean velocity results for both configurations are presented in 3.1 and the turbulence results in 3.2. The measurements in higher concentrations of particles are presented in sub-section 3.3. The results are discussed in section 4 and a list of the

most important findings is given in section 5.

## 2. FLOW CONFIGURATIONS AND MEASUREMENT TECHNIQUES

### 2.1. Flow configurations

The measurements presented in section 3 were made with each of two baffles located in a pipe of 25.4mm diameter situated in the water tunnel shown schematically in Figure 1. The fluid from a constant head tank was supplied to the pipe and the baffles were located 120 diameters downstream of the pipe inlet. The liquid and the solids suspended in it were circulated by a pneumatically-driven flap-valve diaphragm pump, selected specifically so that no particle degradation was caused by the pumping action. A 100mm length of pipe around the measurement station was constructed from Plexiglass to enable optical access. The outside surfaces of the transparent section were made plane so that refraction effects at the air/Plexiglass interface were not as severe as in the presence of a curved surface.

Diakon (Perspex/Plexiglass equivalent, made by ICI plc) transparent particles were used for all the two-phase flow measurements in a carrier phase of water: their properties are listed in Table 2 below. The sink velocities of the particles in the water were small enough (0.3% of the bulk velocity) for the particles to be considered neutrally buoyant.

The loading ratios for the particle concentrations used, i.e. the ratio of the solids mass flow rate to that of the liquid is 0.0044 for the 0.375% by volume concentration, rising to 0.0176 for the maximum concentration of 1.5%.

A useful characteristic parameter is the particle response time which is defined as

$$\tau = \frac{d_p^2 \rho_p}{18\mu}$$

but alternative definitions are also employed, such as

$$\tau = \frac{d_p^2(2\rho_p/(\rho_f+1))}{36\nu}$$

(Wells and Stock, 1983). For the 270$\mu$m mean diameter particles, $\tau$ is about 4ms from both expressions. A corresponding characteristic response time for the flow can be defined in terms of the pipe or baffle diameter and a bulk or annular bulk velocity, yielding values of about 3-10ms. The particles are therefore expected to be able to follow the flow.

TABLE 2 - Material Properties at S.T.P.

| Property | Water | Diakon MH251 |
|---|---|---|
| Density (kg/m$^3$) | 998 | 1,180 |
| Viscosity (Nsm$^{-2}$) | 0.001 | – |
| Refractive index ($n_D^{20}$) | 1.333 | 1.491 |
| Size range ($\mu$m) | – | 180-350 |
| Mean diameter ($\mu$m) | – | 270 |
| Sink velocity in water (mm/s) | – | 7.2 |

The measurements were made at the same pipe Reynolds number (Re) and mass flow rate ($\dot{m}$) with both baffles; the baffle size, bulk velocities and relevant parameters are listed in Table 3. The cone and disc baffle geometries and the corresponding measurement stations are shown in Figures 2(a) and 2(b) respectively.

TABLE 3 - Characteristic flow dimensions and parameters

|  | Cone, 25% blockage | Disk, 50% blockage |
|---|---|---|
| Baffle diameter, $D_b$ (mm) | 12.50 | 17.96 |
| Bulk velocity in pipe, $V_B$(m/s) | 2.04 | 2.04 |
| Annular bulk velocity, $U_o$ (m/s) | 2.72 | 4.08 |
| Pipe Reynolds number, $Re = V_B D/\nu$ | 51,600 | 51,600 |
| Baffle Reynolds number, $Re = U_o D_b/\nu$ | 33,900 | 57,400 |
| Mass flow rate, $\dot{m}$ (kg/s) | 1.0315 | 1.0315 |

## 2.2 The laser-Doppler anemometer and experimental technique

Particles crossing the beam intersection volume in a fringe-type Doppler velocimeter scatter light because of diffraction, reflection and refraction of the incident light beams. As the particle size increases diffraction scatter becomes negligible in comparison to geometric scatter i.e. reflection and refraction (see e.g. Hodkinson and Greenleaves (1963) and van de Hulst (1957)). The two types of particle present in the flows considered here, i.e. transparent solid particles of $270\mu m$ mean diameter and near micron contaminants which follow the flow, result in signals like those of figure 3; $I_{p,p}$ and $I_{p,l}$ are the intensities of the pedestal (d.c.) component of the solid and liquid phase signals and $I_{m,p}$ and $I_{m,l}$ the corresponding a.c. component modulations. It is possible to distinguish therefore the phase measured by the intensity of the scattered light, as $I_{p,p} \gg I_{p,l}$ and $I_{m,p} > I_{m,l}$. The detection of signals from the solid (high intensity) phase only can be made by reducing the photomultiplier sensitivity or by reducing the amount of light incident upon the photomultiplier by means of an adjustable aperture (iris) (Robinson and Chu, 1975) to a level low enough so that the small-intensity (liquid phase)

signals will not be detected. In the present work the mean and turbulence velocities of the liquid phase in single-phase flow and those of the solid particles in two-phase flow were measured.

The laser-Doppler velocimeter is shown schematically in Figures 4(a) (optical system) and 4(b) (signal processing system). The principal characteristics of the optical system are given in Table 4 below. The iris aperture was fully open for the single-phase flow measurements and, once they were completed, was closed to the position where no more signals were detected from the small scatterers and subsequently the Diakon particles were inserted in the flow. The Doppler signals were processed by a frequency counter employing validation circuitry to reject erroneous measurements; the number of signals contributing to each measurement varied from 1,000 to 5,000 depending on the location and the local turbulence intensity. The refraction through the fluid was accounted for in the location of the control volume of the velocimeter.

Sources and estimates of errors for a similar velocimeter used in single-phase flow have been given by Popiolek et al (1984) and are not repeated here. In brief, systematic errors in the mean velocities are of the order of 1%, rising to 2-3% in the steep-gradient regions near the walls. The accuracy of the results can be assessed by integrating the continuum phase velocity profiles at different stations to establish that the mass flow rate is the same at each station and yielded results which were constant to within ±5%; considering the interpolation and integration errors which can result from the steep velocity gradients this figure is consistent with the estimates for the accuracy of the local velocities.

TABLE 4 - Principal characteristics of the optical system

| | |
|---|---|
| Half-angle of beam intersection in air (degrees) | 8.60 |
| Frequency-to-velocity transfer constant (m/s/MHz) | 2.115 |
| Intersection volume diameter calculated at 1/e$^2$ intensity ($\mu$m) | 50 |
| Intersection volume length calculated at 1/e$^2$ intensity ($\mu$m) | 445 |
| Number of fringes in intersection volume without frequency shifting | 24 |
| Fringe separation (line-pair spacing) ($\mu$m) | 2.115 |
| Frequency shift between beams (MHz) | ±1.735 |

The equation for the frequency-to-velocity transfer constant for large particles tends towards the universal equation of laser velocimetry for single phase measurements when the ratio of the distance of the control volume from the photo-detector to the particle radius is large and the beam crossing angle is small (Durst and Zare, 1975), which is the case in the present work.

A characteristic parameter for particle scattering considerations is $\alpha=(\pi d)/\lambda$, where d is the particle diameter and $\lambda$ the wavelength of the incident radiation (van de Hulst, 1957). The two requirements for the use of geometrical optics are that a>>1 and that the index of refraction (n) of the particle differs sufficiently from that of its surroundings (Bachalo, (1980)). As $\alpha\approx10^3$ and $\Delta n\approx10^{-1}$ in the present system the diffractive scatter is sufficiently small to be separated from reflective and refractive scatter.

The ability to measure in the presence of solid particles which block the beams and the light scattered from the control volume depends on the particle concentration (c), $\Delta n$, the length the beams have to travel in the flow (df), and the ratio of the diameter of the particles (dp) to that of

the laser beams. The smaller $\Delta n$, $d_p$ and $df$, the larger the concentration through which the beams will penetrate. In the present system, measurements could be obtained throughout the pipe for particle concentrations up to 1.5%; the signal-to-noise ratio deteriorated with increasing concentration and for a particle content of 3-4% by volume measurements were possible only near the centreline.

## 3. RESULTS

### 3.1 Mean velocity results

The symmetry of the flow was established to be within the precision of the measurements for both configurations; the largest asymmetries of about 5% were encountered in the regions of steep gradients.

The mean velocity profiles measured in the cone and disk baffle configurations are shown in Figures 5(a)-(e) and 6(a)-(e) respectively. The axial components of the liquid velocities in single-phase flow are shown together with the solid-phase velocities for a concentration of particles of 0.375 percent by volume. The measurements presented were made in radial planes located at 0.25, 0.50, 0.75, 1.00 and 3.00 baffle diameters ($D_b$) downstream of the baffle.

The mean velocity results for the cone (25% blockage), Fig. 5, show that the annular jet and the recirculation zone behind the baffle persist until the $z=1.0D_b$ station and the flow recovery is evident at the $z=3.0D_b$ station where the profiles are nearly uniform. The recirculation zone length was determined by measurements along the axis of the pipe to be 16.5mm (0.65D). The velocities in the recirculation zone reach maxima of $0.7V_b$ on the axis at $z=0.75D_b$, while the jet velocities do not exceed $1.7V_b$ at any station.

The single-phase liquid flow and the particle velocities are nearly identical in most parts of the flow, as expected because of the near-neutral buoyancy of the particles. In the recirculation zone the particle velocities are up to 3% smaller than the liquid ones near the axis and the

particle velocities are up to 3% smaller than the liquid ones near the axis and the $\bar{U}_p$ profile is only slightly flatter. The same trend is evident in the jet region near the wall, but with the particle velocities leading the fluid by about $0.02-0.04V_b$. In the downstream station, $z=3.0$ $D_b$, the flow recovery exhibits similar trends as in the upstream region; particle velocities are smaller in the vicinity of the axis and larger near the wall by about $0.05$ $V_b$ in comparison to the single-phase result. As the variation in $\bar{U}_p$ is larger than that in $\bar{U}_p$ this result suggests that the flow recovery is slower in the two-phase situation.

The results for the disc-shaped baffle (50% area blockage) shown in Figure 6(a)-(e) indicate expectedly that the velocity gradients associated with the increased area blockage are larger; velocity maxima in the jet region reach $2.6V_b$ and in the recirculation zone $1.15V_b$. The recirculation zone length was 38.5mm (1.5D) in this configuration. Again the flow recovery is evident at the $z=3.0D_b$ station, but the profile is less uniform than that for the conical baffle (Fig. 5(e)).

A comparison of the single-phase liquid velocities with those of the particles shows similar trends to these of the conical baffle but they are more pronounced in the case of the disc. Particle velocity profiles are flatter both in the jet region near the wall and in the recirculation zone in the vicinity of the axis. Mean velocity differences are no more than $0.1V_b$ on the axis, but larger differences are found near the centre of the recirculation zone. In the jet region particle velocities in general lag by about $0.01-0.03V_b$ behind those of the single-phase. The results at the downstream section show the particle velocities lagging behind the fluid ones across the radius of the pipe. The results for the disc baffle suggest that due to the larger accelerations and decelerations of the flow and rapid flow direction changes the particles follow less faithfully than in the cone configuration. The jet width appears to be smaller in the two-phase case.
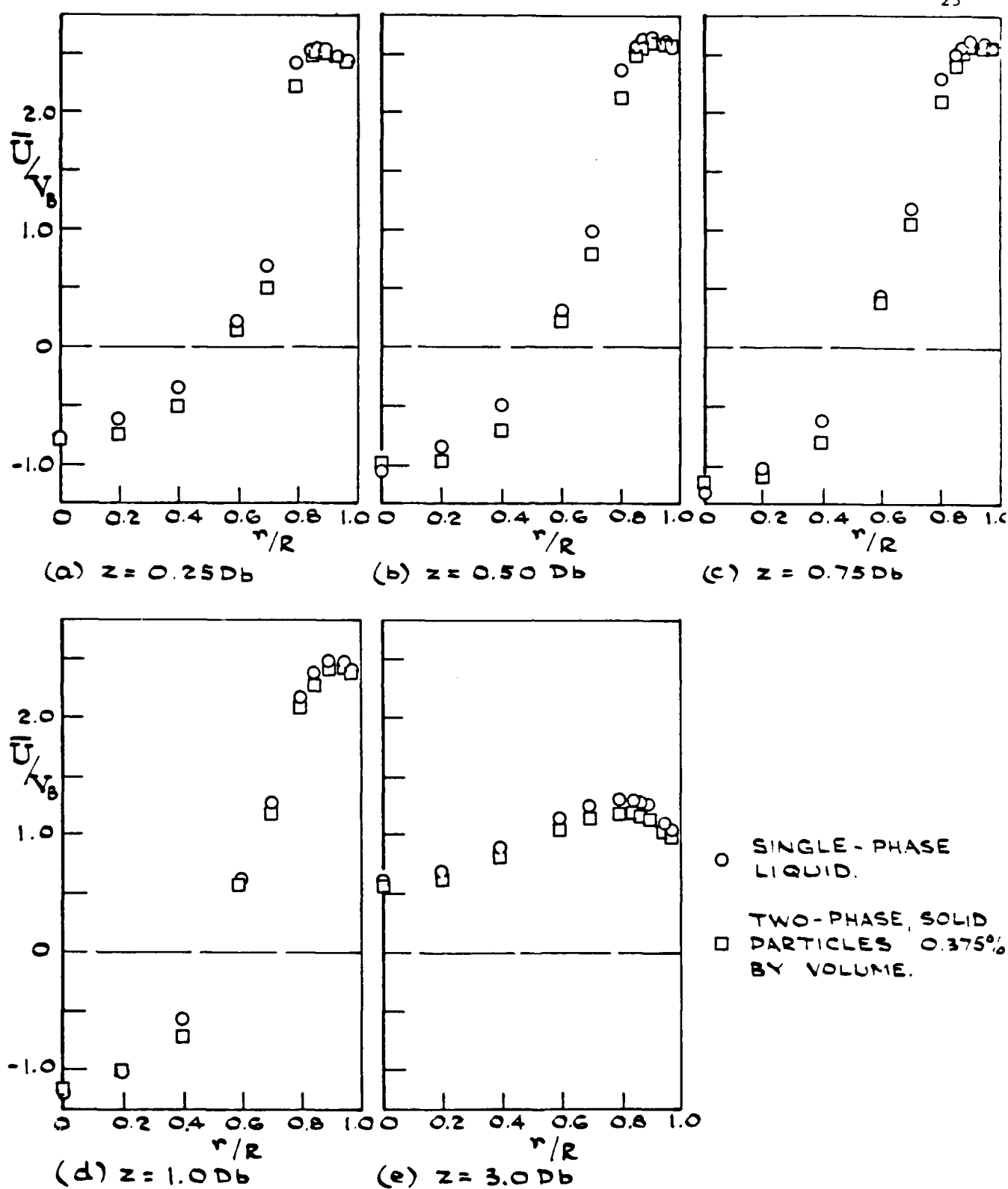
(a) z = 0.25 Db

(b) z = 0.50 Db

(c) z = 0.75 Db

(d) z = 1.0 Db

(e) z = 3.0 Db

○ SINGLE - PHASE LIQUID.

□ TWO - PHASE, SOLID PARTICLES 0.375% BY VOLUME.

Fig. 6  Profiles of $\bar{U}/V_B$ with disc

(a) z = 0.25 Db

(b) z = 0.50 Db

(c) z = 0.75 Db

(d) z = 1.0 Db

(e) z = 3.0 Db

O SINGLE-PHASE LIQUID

□ TWO-PHASE, SOLID PARTICLES 0.375% BY VOLUME

Fig. 5  Profiles of $\bar{U}/V_B$ with cone

TO
SIGNAL
PROCESSING
SYSTEM

DIMENSIONS IN mm

RADIAL
DIFFRACTION
GRATING

417    135                300        60

PHOTOMULTIPLIER

PINHOLE

IRIS

MASK

COLLECTING LENS

TEST
SECTION

MASK

IMAGING
LENS

COLLIMATING
LENS

5mW HeNe
LASER

(a) Optical system

AMPLIFIER

BANDPASS
FILTER

OSCILLOSCOPE

PM

a

b

FREQUENCY
COUNTER

MICROPROCESSOR

VDU

(b) Signal processing system

Fig. 4 Laser-Doppler anemometer
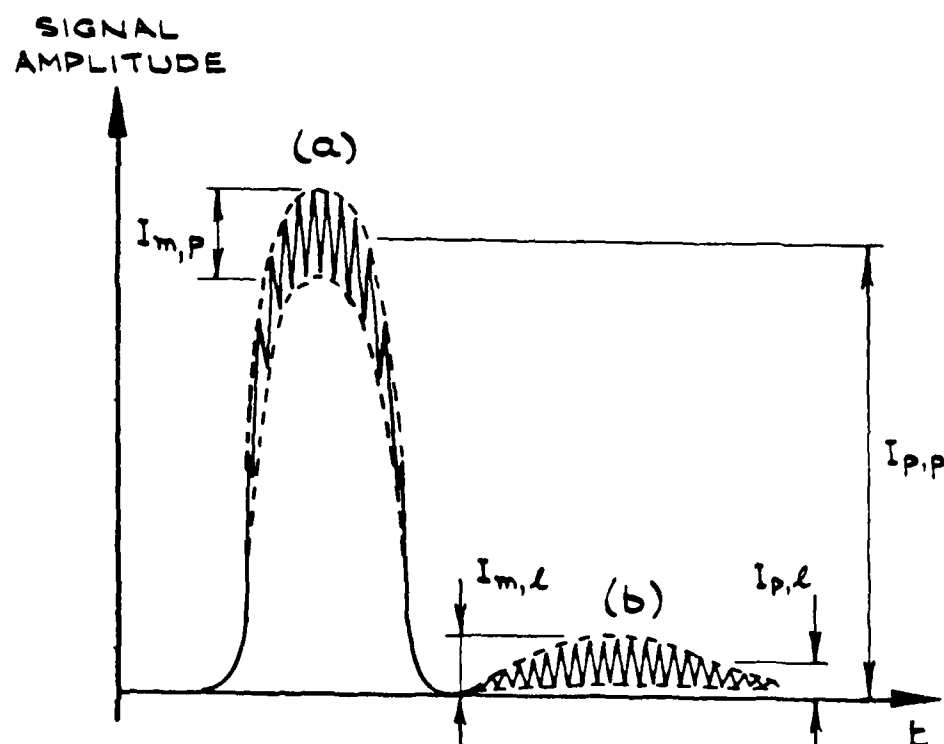
Fig. 3 Characteristic Doppler signals from
(a) the solid particles and
(b) the micron-size particles following the
fluid motions
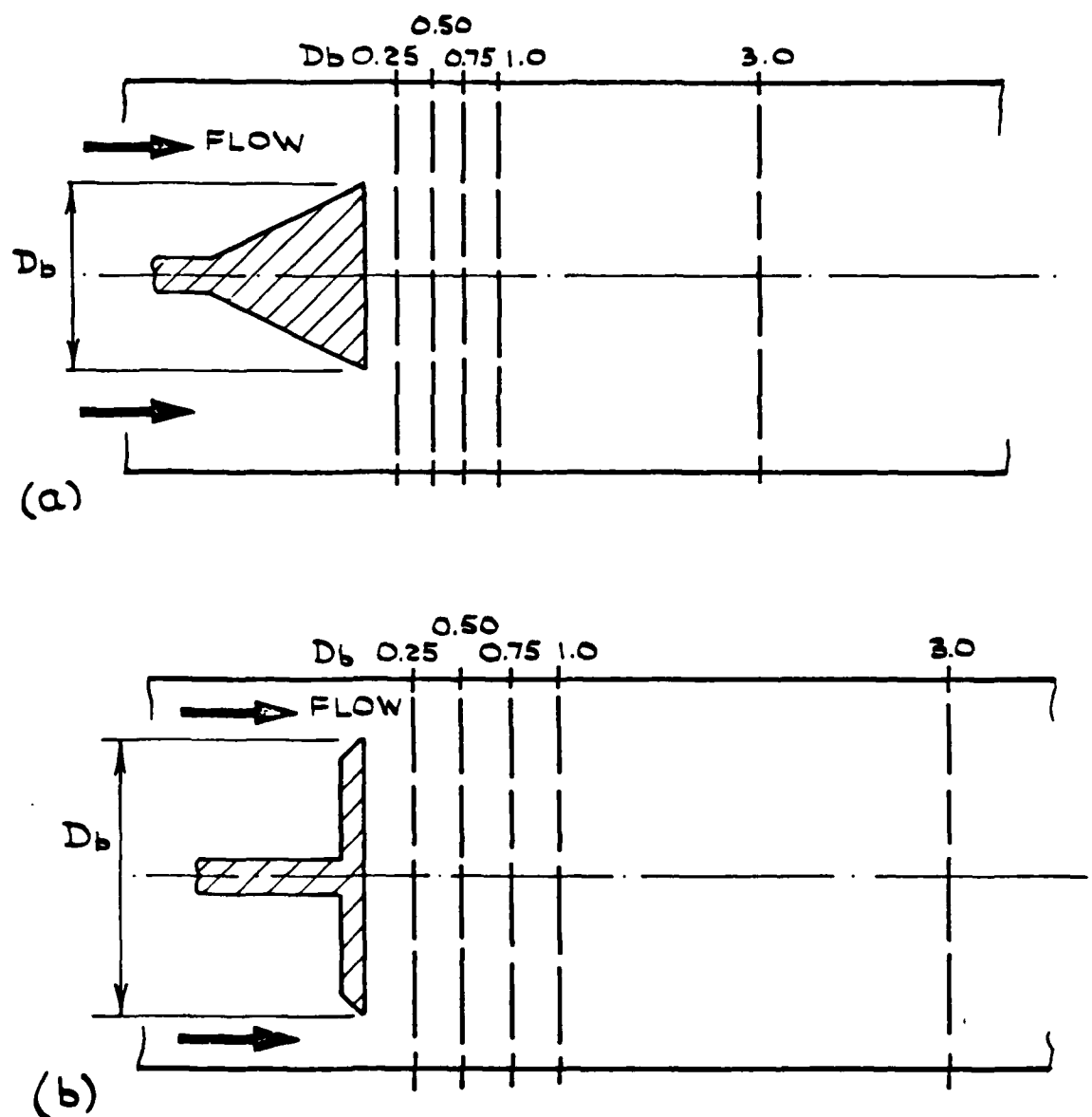
Fig. 2  Diagram of baffles and location of measurement stations:
(a) Cone, 25% area blockage,  (b) disc, 50% area blockage
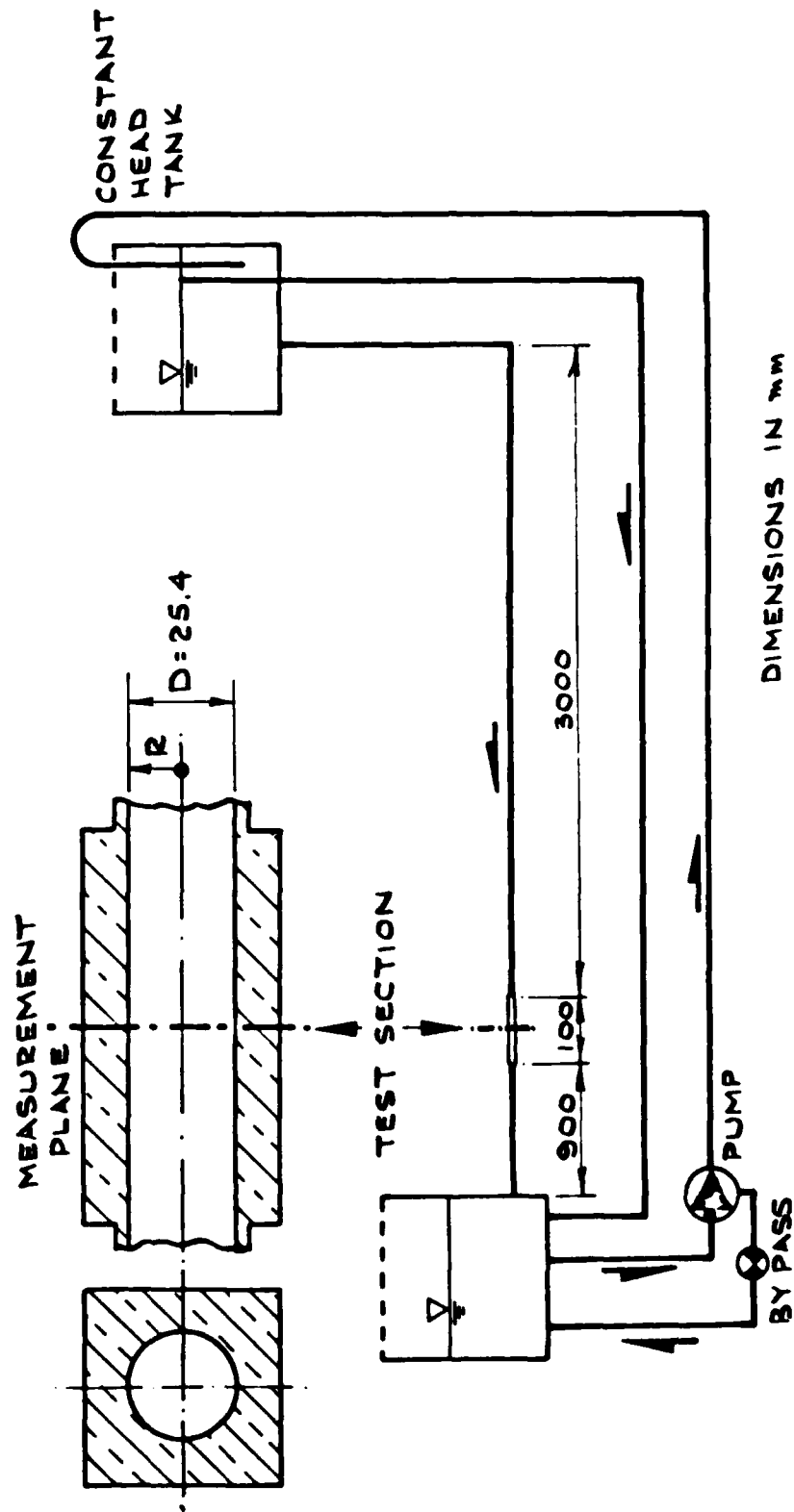
Fig. 1 Schematic diagram of water tunnel

Tsuji, Y., Morikawa, Y. and Shiomi, H. (1984). LDV measurements of an air-solid two-phase flow in a vertical pipe. J. Fluid Mech., 139, 417.

van de Hulst, H.C. (1957). Light scattering by small particles. Dover Publications, New York.

Wells, M.R. and Stock, D.E. (1983). The effects of crossing trajectories on the dispersion of particles in turbulent flow. J. Fluid Mech., 136, 31.

Zisselmar, R. and Molerus, O. (1978). Investigation of solid-liquid pipe flow with regard to turbulence modification. Int. Symposium on Momentum, Heat and Mass Transfer in Two-Phase Engergy and Chemical Systems, Dubrovnik, Yugoslavia, 4-9 September 1978.

Popiolek, Z., Whitelaw, J.H. and Yianneskis, M. (1984). Unsteady flow over disc turbine blades. Proc. 2nd Symp. on Applications of Laser Anemometry to Fluid Mechanics, Lisbon, July 1984.

Robinson, D.M. and Chu, W.P. (1975). Diffraction analysis of Doppler signal characteristics for a cross-beam laser-Doppler velocimeter. Applied Optics, 14, 2177.

Soo, S.L. (1967). Fluid dynamics of multiphase systems. Blaisdell Publishing Co., Waltham, Mass.

Soo, S.L., Trezet, G.J. Dimick, R.C. and Hohnstreiter, G.F. (1964). Concentration and mass flow distribution in a gas-solid suspension. Ind. Eng. Chem. Fundamentals, 3, 98.

Steinour, H.H. (1944). Nonflocculated suspensions of uniform spheres. Ind. Eng. Chem., 36, 618.

Taylor, A.M.K.P. and Whitelaw, J.H. (1984). Velocity characteristics in the turbulent near wakes of confined axisymmetric bluff bodies. J. Fluid Mech., 139, 391.

Tridimas, Y.D., Hobson, C.A., Wooley, N.H. and Lalor, M.J. (1982). Measurement of the velocities of the two phases in a flowing gas solid suspension using LDA. Proc. First Symp. on Applications of Laser Anemometry to Fluid Mechanics, Lisbon, July 1982.

Tsuji, Y. and Morikawa, Y. (1982). LDV measurements of an air-solid two-phase flow in a horizontal pipe. J. Fluid Mech., 120, 385.

Hodkinson, J.R. and Greenleaves, I. (1963). Computations of light-scattering and extinction by spheres according to diffraction and geometrical optics, and some comparisons with the Mie theory. J. Opt. Soc. Amer., 53, 577.

Kaye, B.H. and Boardman, R.P. (1962). Cluster formation in dilute suspensions. Proc. of Symposium on interaction between fluids and particles, I. Chem. E., London.

Lee, S.L. and Durst, F. (1982). On the motion of particles in turbulent duct flows. Int. J. Multiphase Flow, 8, 125.

Levy, Y. and Lockwood, F.C. (1981). Velocity measurements in a particle laden turbulent free jet. Comb. and Flame, 40, 333.

Looney, K. (1983). Private communication.

Modarress, D., Wuerer, J. and Elgobashi, S. (1982). An experimental study of a turbulent round two-phase jet. AIAA/ASME 3rd Joint Thermophysics, Fluids, Plasma and Heat Transfer Conference, St. Louis, 7-11 June 1982.

Newitt, D.M., Richardson, J.F. and Shook, C.A. (1962). Hydraulic conveying of solids in horizontal pipes. Part II: distribution of particles and slip velocities. Proc. Symp. on interaction between fluids and particles. I. Chem. E., London.

Owen, P.R. (1969). Pneumatic transport. J. Fluid Mech., 39, 407.

## REFERENCES

Abbott, M. (1955). The hydraulic conveying of solids in pipelines. Ph.D. Thesis, University of London.

Bachalo, W.D. (1980). Method for measuring the size and velocity of spheres by dual-beam light-scatter interferometry. Appl. Optics, 19, 363.

Birchenough, A. and Mason, J.S. (1976). Laser anemometry measurements in a gas-solid suspension flow. Optics and Laser Technology, 8, 253.

Choi, Y.D. and Chung, M.K. (1983). Analysis of turbulent gas-solid suspension flow in a pipe. Proc. ASME Conference, Houston, June 20-22 1983, Paper no. 83-FE-6.

Cox, P. and Mason, S. (1975). Flow of fluids in pipes in the presence of suspended particles. Rheology of suspensions.

Durst, F. and Zare, M. (1975). Laser-Doppler measurements in two-phase flows. Proc. of the LDA-Symposium, Univ. of Denmark, Copenhagen.

Einav, S. and Lee, S.L. (1973). Particles migration in laminar boundary layer flow. Int. J. Multiphase Flow, 1, 73.

Grossman, A.G. (1981). The flow of moderately concentrated suspensions in the Stokes approximation. Fluid Mechanics - Soviet Research, 10, 5, 96.

Hetsroni, G. and Sokolov, M. (1971). Distribution of mass, velocity and intensity of turbulence in a two-phase turbulent jet. J. Appl. Mech., June 1971, 315.

qualitative agreement with the result of Zisslemar and Molerus (1978), who reported a 12% reduction of turbulence levels in pipe flow in the presence of 53μm diameter particles in a concentration of 1.7% by volume.

## 5. CONCLUDING REMARKS

1. Measurements of the streamwise mean and r.m.s. velocity components were presented for the two-phase flow of 270μm mean diameter solid particles in water behind two axisymmetric baffles, a conical baffle of 25% area blockage and a disk-shaped baffle of 50% area blockage, for particle concentrations up to 1.5% by volume.

2. The mean velocity results show that for a concentration of solids of 0.375% by volume the particles in general follow the fluid motion behind the conical baffle but the annular jet region behind the disc-shaped baffle is narrower in the presence of the particles; in the recirculation zone the particle velocity profiles are flatter than those in single-phase flow.

3. The measured turbulence levels in the presence of the particles are consistently lower than those of the fluid in single-phase flow. This suppression of turbulence varies in magnitude from 3-38% depending on the location in the flow.

4. Measurements were made in both configurations with varying concentrations of particles of up to 1% in the disk and up to 1.5% in the cone configuration, and showed that the particle turbulence levels decreased as the concentration was increased.

z=0.75 R and 1.07 R.   The two sets of results are qualitatively and quantitatively similar except that the mean square levels in the recirculation zone, Fig. 11(c), differ because of the axial location of the present profiles.

The mean flow results show that there are small differences ($^\sim$0.04$V_b$) in the solid and liquid velocities only in regions where there is considerable acceleration or deceleration of the flow as expected. Calculations by Looney (1983) have shown that in one-dimensioanl flow of identical Diakon particles in water there is negligible slip between the two phases for 0.5 and 1.0% concentrations of solids.  The present result is also in agreement with the observations of Cox and Mason (1975) for neutrally buoyant particles.   Newitt et al (1962) have also shown experimentally that for the flow of particles of 0.1-0.2mm in diameter in water flow in a 0.0254m diameter pipe there was no local slip between the liquid and particle velocities: their observations included the flow of 0.18mm diameter Diakon particles.

The particle mean velocity profiles have also been found to be flatter than the single-phase fluid velocity profiles by Birchenough and Mason (1976), Lee and Durst (1982), Tridimas et al (1982) and others.   The flattening of the particle velocity profile as the solids concentration or mass loading is increased (Fig.  9(a) and (b)) has been reported by Tsuji and Morikawa (1984) and, for the flow of liquid droplets in air, by Betsroni and Sokolov (1971).  Lee and Durst (1982) and Tsuji and Morikawa (1984) have reported that particles of 200$\mu$m diameter have higher velocities than the fluid in the near-wall region in pipe flow.  In the present results this was observed in the cone configuration but not in the disc one where the addition of the particles affects the shape of the annular jet.

The r.m.s. velocity results indicate that turbulence is in general suppressed in the presence of the particles.  The reduction in turbulence levels by about 5% observed in the recovering flow at z=3.0$D_b$ is in

the signal-to-noise ratio deteriorated significantly and the validated data rate was unacceptably low. The profile of the particle velocities becomes flatter in the jet region as the concentration is increased but there are no discernable trends in the recirculation region. Figure 9(b) shows the corresponding results in the disc configuration for particle concentrations of up to 1%. In this case the $\bar{U}_p$ profiles are again becoming increasingly flatter with concentration both in the jet and in the near-axis region. The steep velocity gradient at mid-radius is found nearer the wall as the concentration is increased.

The turbulence levels are shown in Figures 10(a) and (b). In the conical baffle case the reduction in turbulence levels becomes bigger as the concentration is increased. The same trend is observed for the disc (Fig. 10(b)), but in the near-wall region the particle turbulence levels are in places higher than those of the fluid, probably due to the relative change of the size of the jet region.

4. DISCUSSION

The present single-phase results may be compared with those obtained by Taylor and Whitelaw (1984) for two identical configurations in a test section twice the size of the present one, see Figures 11(a), (b) and (c). The centreline profiles of axial velocity are shown in Fig. 11(a) and indicate that the cone results are practically identical, but there are small differences at $z/R \approx 2.5$ for the disc results, which probably stem from differences in the details of the geometry upstream of the baffle. The recirculation zone lengths are the same in both cases. Comparison of the radial profiles of the mean and r.m.s. velocities are shown for the cone (Fig. 11(b)) and for the disc (Fig. 11(c)). The comparison is made with the results of Taylor and Whitelaw in stations located at $z=0.6$ R and 1.19 R for the cone and disc respectively while the present results were taken at

## 3.2  Turbulence level results

The r.m.s. velocities or turbulence levels corresponding to the mean results of Figures 5 and 6 are shown in Figures 7(a)-(e) and 8(a)-(e) respectively.  The results for the conical baffle show that turbulence is suppressed in comparison with the single-phase flow levels.  The reduction in turbulence levels is about 10-38% in the wall region, 5-17% in the jet region 5-25% in the recirculation and 5-13% on the axis.  The biggest suppression of turbulence takes place at 0.5 and 0.75 $D_b$ where the single-phase levels are higher.  In the downstream station, Fig. 7(e), the difference in levels across the radius is about 5%, indicating the flow recovery in the turbulence structure as well.

The turbulence levels for the disc-shaped baffle show similar trends (Fig. 8(a)-(e)) but the levels are higher (by about 40%) due to the larger velocity gradients and the greater generation of turbulence involved.  The suppression of turbulence is not as pronounced as with the cone; particle turbulence levels are 4-17% lower near the wall and 4-13% lower near the axis.  In the region of the steep velocity gradient the levels are sometimes higher than those of the single-phase: the steep velocity gradient is found nearer the wall in the two-phase case (indicating a narrower jet region and a wider recirculation zone) resulting in that the peak in the turbulence level profile is located nearer the wall also.

## 3.3  Results with higher particle concentrations

The mean and r.m.s. velocities were measured in both configurations with increasing void fractions of particles to establish the effect of concentration on the mean and turbulence structure.  Results at z=1.0 $D_b$ are shown in Figures 9 and 10.

Mean velocities are shown in Figure 9(a) for particle concentrations of up to 1.5% by volume in the cone configuration.  At higher concentrations
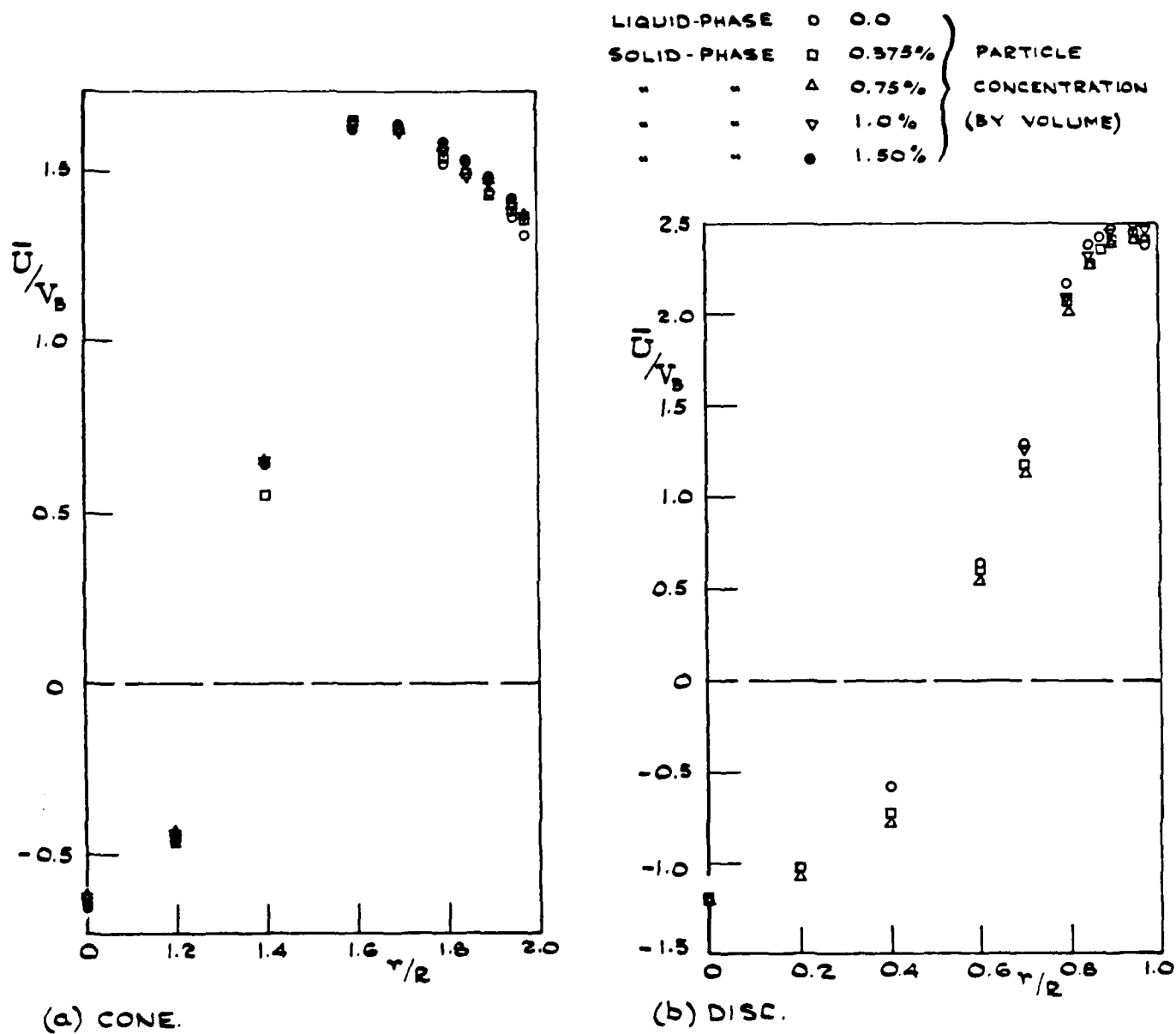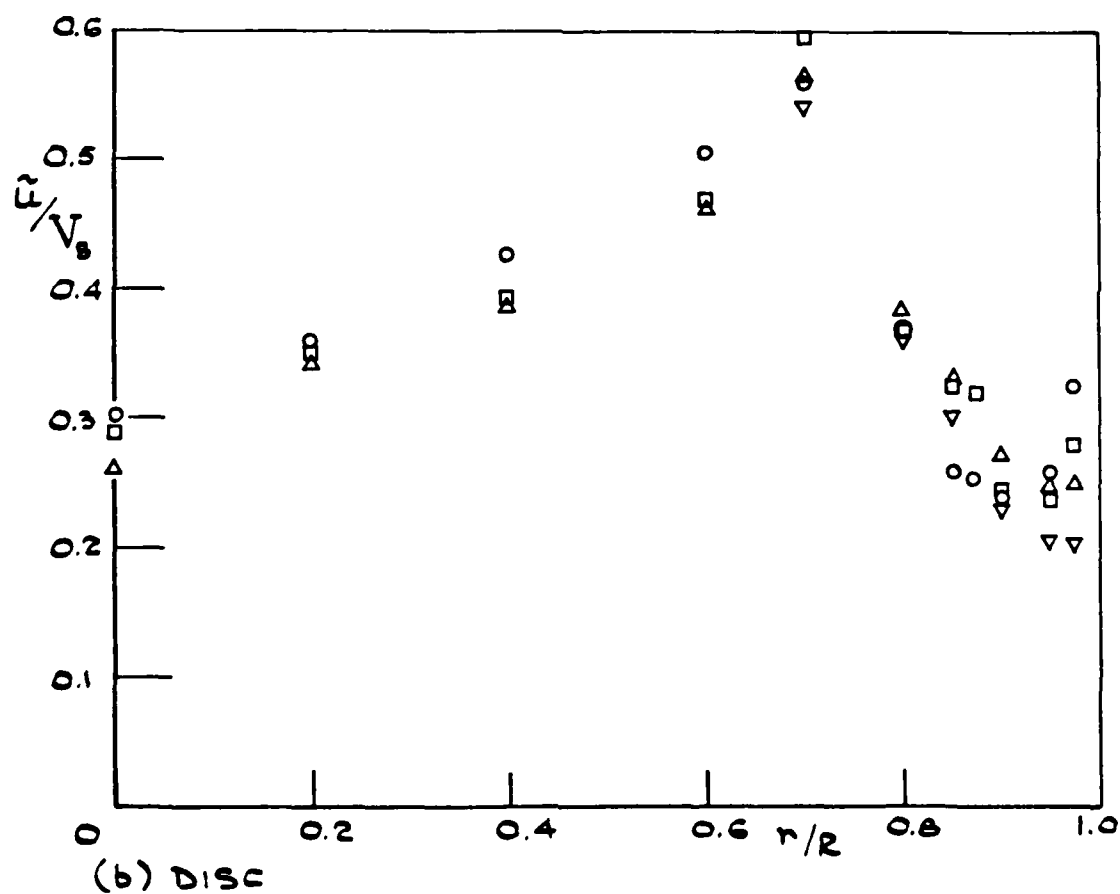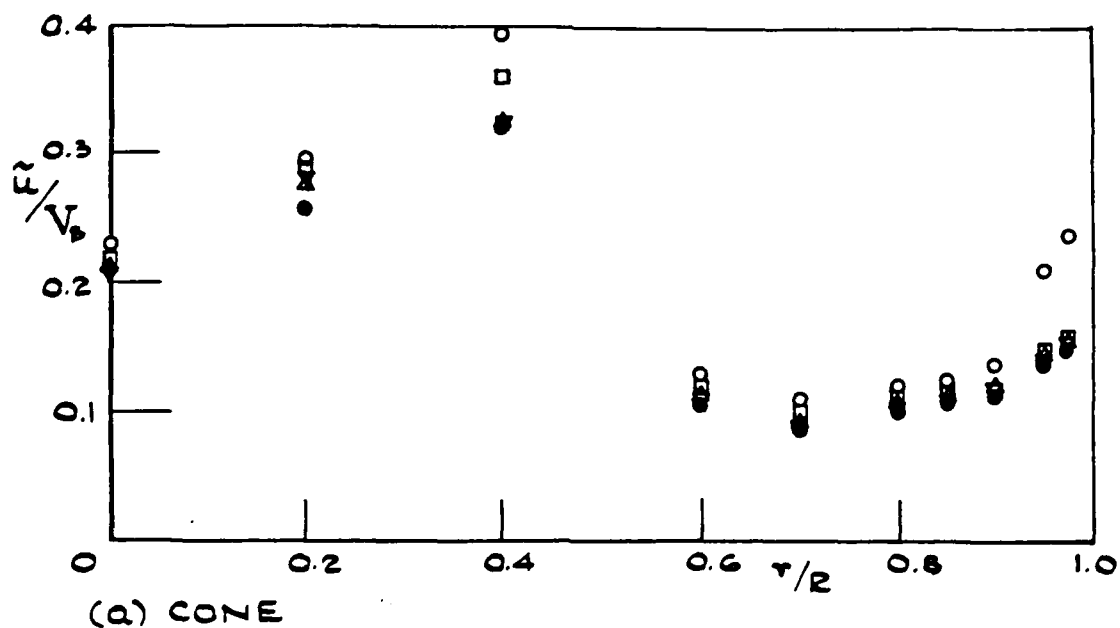
Fig. 7 Profiles of $\bar{u}/V_B$ with cone

O SINGLE-PHASE, LIQUID
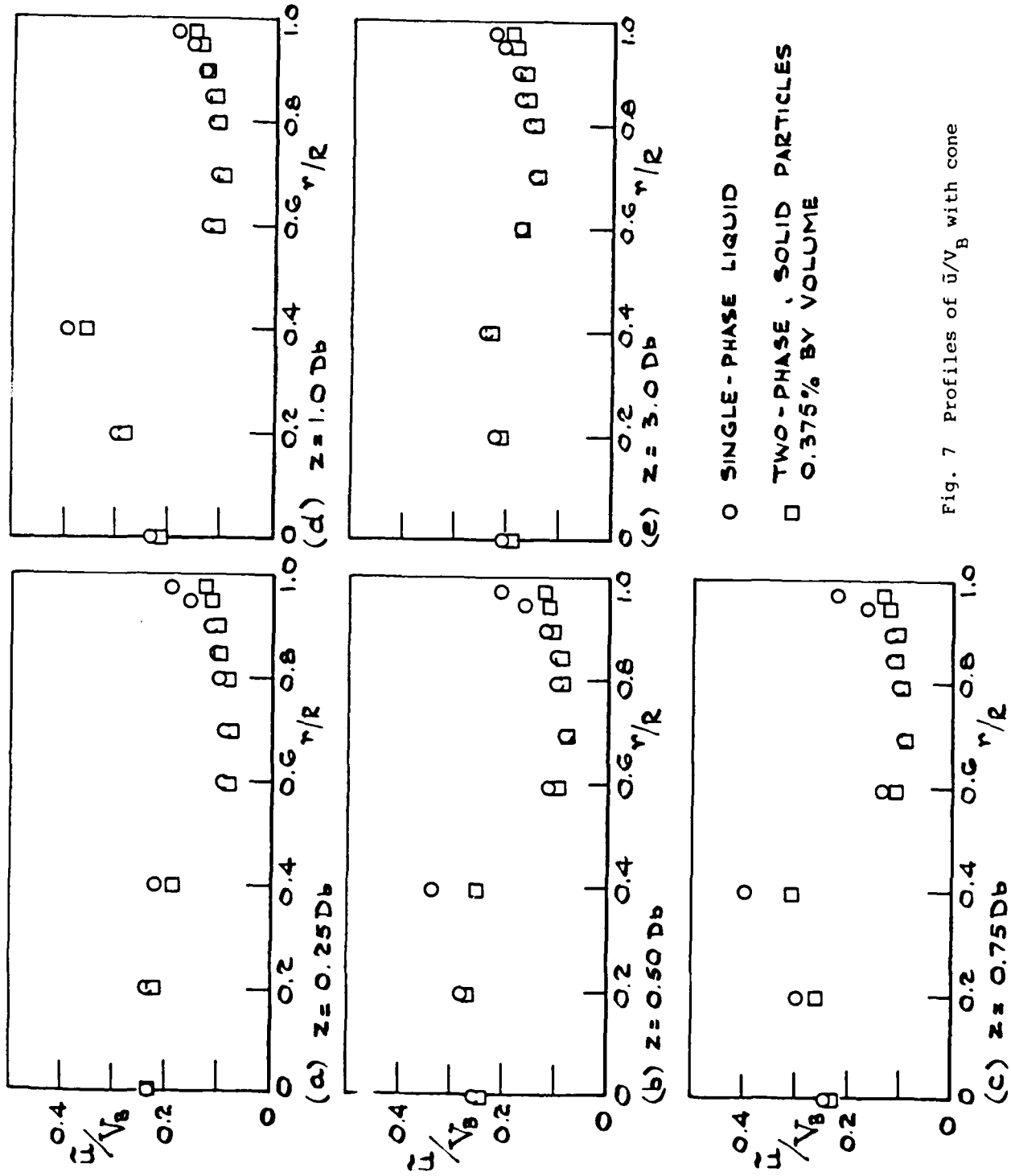
□ TWO-PHASE, SOLID PARTICLES, 0.375% BY VOLUME.
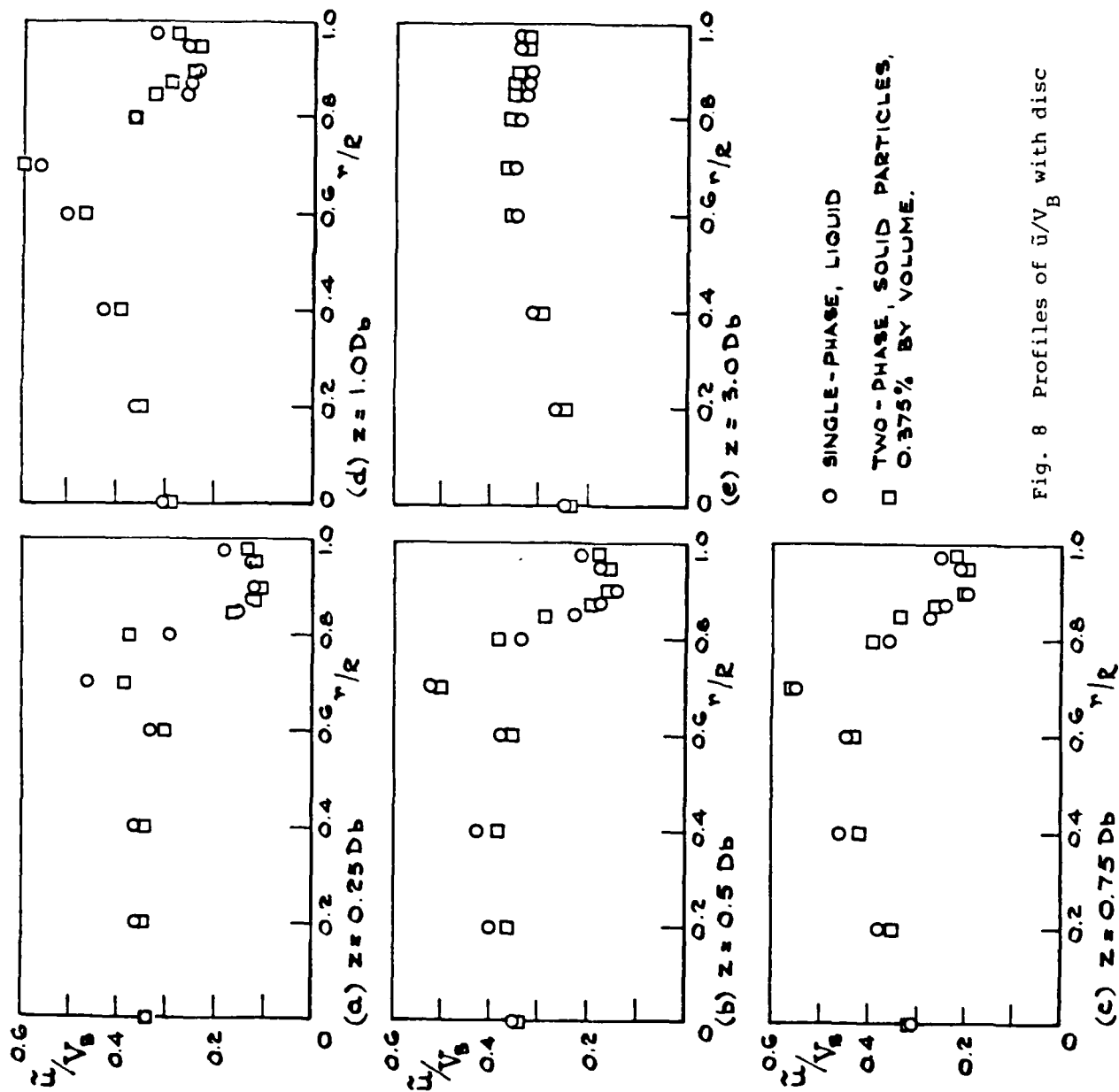
Fig. 8  Profiles of $\tilde{u}/V_B$ with disc

Fig. 9  Profiles of $\bar{U}/V_B$ at $z = 1.0\ D_b$ for various concentrations of solids

(a) CONE

(b) DISC

| LIQUID - PHASE | o | 0 % | |
|---|---|---|---|
| SOLID - PHASE | □ | 0.375% | } PARTICLE |
| " | △ | 0.75% | CONCENTRATION |
| " | ▽ | 1.0% | (BY VOLUME) |
| " | ● | 1.5% | |

Fig. 10   Profiles of $\tilde{u}/V_B$ at $z = 1.0\ D_b$ for various concentrations of solids
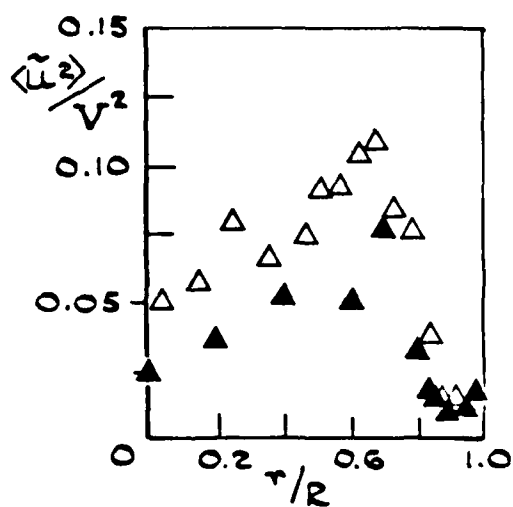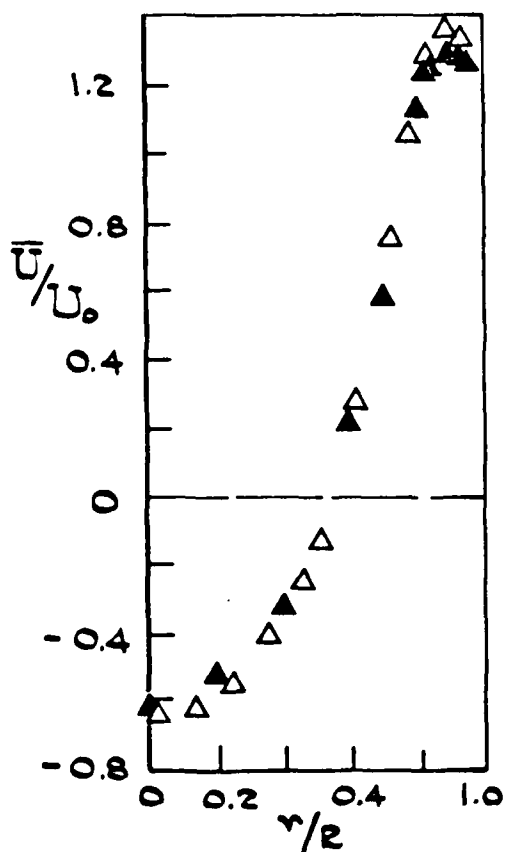
Fig. 11 (a) Centre-line profiles of $\bar{U}/U_o$ for the cone and disc configurations

■ THIS WORK

□ TAYLOR & WHITELAW (1984)
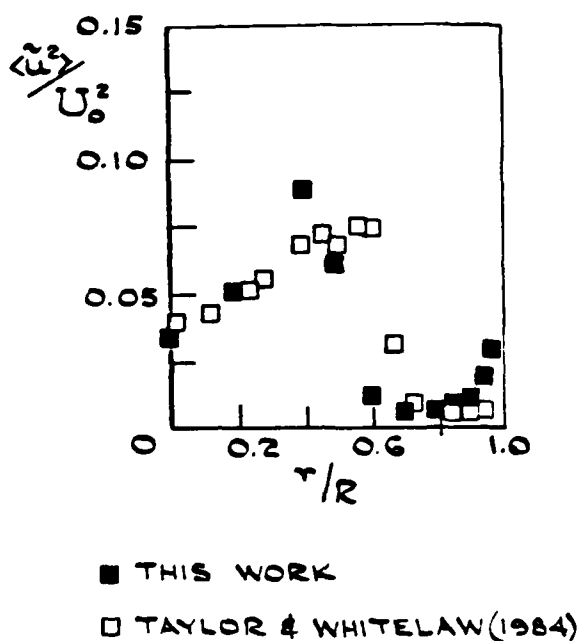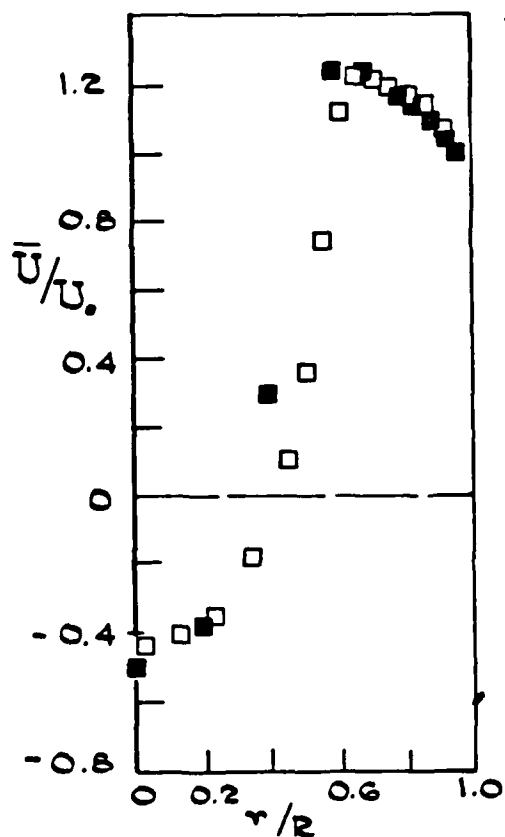
(b) CONE

▲ THIS WORK

△ TAYLOR & WHITELAW (1984)

(c) DISC

Fig. 11 (b) and (c)   Radial profiles of $\bar{U}/U_o$ and $<\tilde{u}^2>/U_o$ for the cone and disc configurations